

Spin-dependent electronic transport properties of liquid manganese

H. Zroui,^{1,2} J. Hugel,¹ A. Makradi,¹ and J. G. Gasser^{1,*}

¹*Laboratoire de Physique des Liquides et des Interfaces, Université de Metz, 1 Boulevard Dominique François Arago, Case Postale 87811, 57078 Metz Cedex 3, France*

²*Laboratoire de Physique du Solide, Département de Physique, Faculté des Sciences, Université Mohammed I, Oujda, Morocco*
(Received 15 March 2001; published 8 August 2001)

The experimental resistivity ρ and thermopower S of liquid manganese have been interpreted within the framework of the extended Ziman formalism for both spin-independent and spin-dependent potentials. It appears that the spin-polarized treatment leads to results in much better agreement with the experimental values than the classical spin-independent approach.

DOI: 10.1103/PhysRevB.64.094202

PACS number(s): 72.15.Cz, 71.22.+i, 72.15.Jf, 72.15.-v

I. INTRODUCTION

In simple metals, the electrical current is considered to be carried in an s - p conduction band and the electronic transport properties are well described by the nearly free-electron theory. However, for transition metals or alloys, the situation is less clear owing to the presence of d electrons. The original Ziman theory¹ was extended by Evans, Greenwood, and Lloyd² to apply to liquid noble and transition metals. They simply replace the weak-ion pseudopotential in the Ziman theory¹ by the t matrix determined using the muffin-tin approximation expressed in terms of the phase shifts. Within the extended Ziman formalism, two approaches have been developed. One has been initiated by Dreirach *et al.*³ and the other by Esposito, Ehrenreich, and Gelatt.⁴ The difference lies in the fact that the former includes only s electrons to form the conduction band whereas the latter takes into account the s and d electrons. Both approaches do not make any difference between the majority (spin-up) and the minority (spin-down) electronic potentials when the atoms bear magnetic moments randomly oriented like in the liquid paramagnetic phase.

The aim of the paper is to show that, for liquid manganese, better results are obtained for the resistivity and thermopower within a spin-polarized approach than within a spin-independent one. *Ab initio* total energy calculations⁵ performed for the solid manganese δ phase below the melting temperature show that two magnetic solutions are possible. A ferromagnetic one with a magnetic moment of $2.7\mu_B$ per atom and an antiferromagnetic one with a moment amounting $3\mu_B$, the latter being favored for minimal energy reasons. In the liquid phase the atoms remnant the solid situation in the sense that they keep their magnetic moment. Since the paramagnetic phase does not exhibit a net magnetization, it is of common use not to take into account the spin of the electron. As a result each electronic state is doubly occupied and all the electrons are subjected to the same potential. For the transport properties, expressed within the scattering theory, the local potentials on the successive sites have to be considered. The individual potentials lead to two scattering channels due to the imbalance between the spin-up and spin-down electrons when a spin moment is located on the site. Presently the resistivity and thermoelectric power are calculated within the above assumption and compared to

the nonmagnetic situation. We use the extended Ziman formalism and obviously we take into account the d electrons.

In Sec. II the extended Ziman theory is summarized together with the relevant parameters. The calculated resistivity and thermoelectric power within the local density approximation (LDA) [Ref. 6] and within the generalized gradient approximation (GGA) as proposed by Perdew, Burke, and Ernzerhof (PBE) (Ref. 7) are presented in Sec. III. The magnetic and nonmagnetic results are discussed in Sec. IV.

II. THEORY

The electrical resistivity of a liquid metal is expressed as a function of the energy E and wave vector k after the Ziman¹ formula, which writes,

$$\rho(E) = \frac{3\pi m_e^2 \Omega_0}{4e^2 \hbar^3 k^6} \int_0^{2k} a(\mathbf{q}) |t(q, E)|^2 q^3 dq, \quad (1)$$

Ω_0 is the atomic volume, q is the transfer wave vector, $a(q)$ is the structure factor which is calculated with hard-spheres model in this work. The hard-spheres structure factor fits very well on the experimental one for liquid manganese with a packing fraction of 0.45; $t(q, E)$ is the t matrix expressed in terms of phase shifts:^{3,8}

$$t(q, E) = - \frac{2\pi \hbar^3}{m \sqrt{2me} \Omega_0} \sum_l (2l+1) \times \sin \eta_l(E) \exp[i \eta_l(E)] P_l(\cos \theta), \quad (2)$$

where $P_l(\cos \theta)$ are the Legendre polynomials, and where θ is the angle between the incident and the scattered wave vector. The phase shifts $\eta_l(E)$ are calculated from muffin-tin potentials determined following the method of Mukhopadhyay, Jain, and Ratti.⁹ If the energy-dependent phase shifts are known, this approach gives an energy-dependent resistivity and allows the calculation of the thermopower as follows:

$$S(E) = - \frac{\pi^2 k_B^2 T_k}{3|e|E} \chi \quad \text{with} \quad \chi = - \left[\frac{\partial \ln \rho(E)}{\partial \ln E} \right], \quad (3)$$

where k_B is the Boltzmann constant, T_K the absolute temperature in Kelvin, and χ the dimensionless thermoelectric parameter.

Within our assumption, the potential felt by an electron of spin up differs from the one seen by an electron of spin down. It gives rise to a two-band conduction mechanism. The formula (1) written for the electron of spin α ($\alpha = \text{up or down}$) becomes

$$\rho^\alpha(E) = \frac{3\pi m_e^2 \Omega_0}{2e^2 \hbar^3 k^6} \int_0^{2k} a(q) |t^\alpha(q, E)|^2 q^3 dq \quad (4)$$

where

$$t^\alpha(q, E) = -\frac{2\pi\hbar^3}{m\sqrt{2me}\Omega_0} \sum_l (2l+1) \times \sin \eta_l^\alpha(E) \exp[i\eta_l^\alpha(E)] P_l(\cos \theta). \quad (5)$$

The phase shifts $\eta^\alpha(E)$ are calculated from muffin-tin potentials for each spin direction. The total resistivity is simply expressed as

$$\frac{1}{\rho} = \frac{1}{\rho^{\text{up}}} + \frac{1}{\rho^{\text{down}}}. \quad (6)$$

The construction of the muffin-tin potentials has been given by Mattheiss¹⁰ for solids and has been adapted to (disordered) liquid metals by Mukhopadhyay, Jain, and Ratti.⁹ Three levels of approximations are used. The first one is the Slater¹¹ x-alpha approximation with only the exchange effects and with the value of alpha (α) taken from Kohn-Sham (KS) theory.¹² The difference between the two approximations appears in the α exchange parameter since it reduces from a value 1 (Slater) to 2/3 (KS). The second approximation takes into account the correlation effects and corresponds to the widely used LDA approximation.⁶ The last approximation includes nonlocal effects via the gradient of the density and is known as GGA. The recent GGA approximation derived by PBE [Ref. 7] has been adopted.

The Fermi energy calculation used in this work was that proposed by Esposito, Ehrenreich, and Gelatt.⁴ The position of E_F , with respect to the scattering muffin-tin zero potential, depends on the shape of the integrated density of states $N(E)$ that has been determined following Lloyd's¹³ method. Esposito, Ehrenreich, and Gelatt⁴ introduced the number of conduction electrons per atom N_C (effective valence) that is different from the valence Z . The Fermi energy is obtained by filling the density-of-states curve by Z electrons per atom, Z being the number of $d+s$ electrons of the conduction band. The Fermi wave vector k_F is obtained from $E_F[k_F = (2mE_F)^{1/2}/\hbar]$, N_C is obtained from k_F ($N_C = k_F^3 \Omega_0 / 3\pi^2$). The two approaches are schematically compared in Fig. 1.

To include the spin effect, the Lloyd formula will be written for the electrons of spin α ($\alpha = \text{up or down}$) as follows:

$$N_\alpha(E) \approx N_0(E) + \frac{2}{\pi} \sum_l (2l+1) \eta_l^\alpha(E), \quad (7)$$

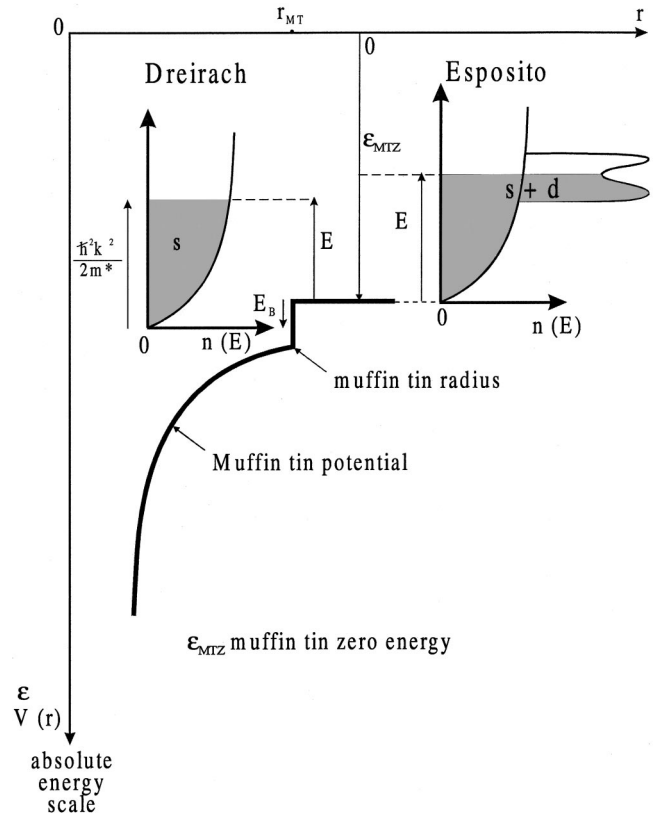


FIG. 1. Schematic density of states and muffin-tin potential on the same energy scale. Dreirach's (Ref. 3) and Esposito's (Ref. 4) approaches. We call E the energy relative to the muffin-tin zero potential and ε the energy on an absolute scale.

where $N_0(E)$ is the free-electron integrated density of states irrespective of the spin direction and $\eta_l^\alpha(E)$ the energy-dependent phase shift for the α spin direction.

The total integrated density of states is

$$N(E) = \frac{1}{2} [N_{\text{up}}(E) + N_{\text{down}}(E)]. \quad (8)$$

III. RESULTS

The spin-independent resistivity curves performed with the Kohn-Sham,¹² LDA (Ref. 6) and GGA-PBE (Ref. 7) approximations are presented in Fig. 2. Calculated and experimental quantities at the Fermi energy are reported in Table I. We observe that the Kohn-Sham potential leads to a very large calculated resistivity (1430 $\mu\Omega$ cm compared to the experiment value of 205 $\mu\Omega$ cm [Ref. 14]). A comparable discrepancy has been evidenced by Esposito Ehrenreich, and Gelatt⁴ for liquid iron since the calculated value of 1130 $\mu\Omega$ cm for the resistivity is widely beyond the experimental value of 136 $\mu\Omega$ cm. It appears that the LDA and GGA curves are very close but largely above the experimental values. Further, the GGA introduced to take care of the inhomogeneity of the electron density does not significantly improve the resistivity of liquid manganese. The energy dependence thermoelectric power curves are shown drawn in Fig. 3. A paper of Vedernikov¹⁵ indicates an experimental thermopower of liquid manganese decreasing with tempera-

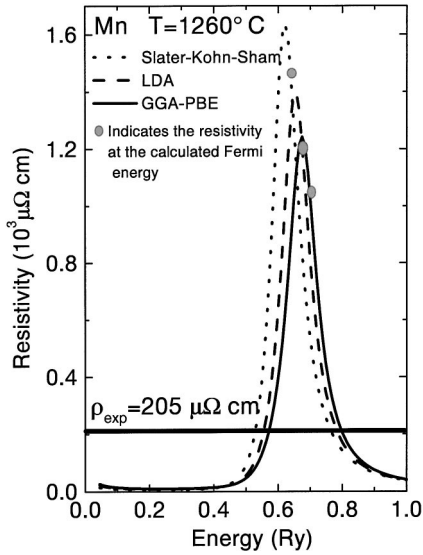


FIG. 2. Energy dependence of the electrical resistivity of liquid manganese. Calculations were made at 1260 °C using the Kohn-Sham (Ref. 12), the LDA (Ref. 6), and GGA-PBE (Ref. 7) potentials without spin effect.

ture from $-0.5 \mu\text{V } ^\circ\text{C}^{-1}$ at the melting point to $-2 \mu\text{V } ^\circ\text{C}^{-1}$, 50 °C above the melting point. An other information can be obtained from an extrapolation of $\text{In}_{1-x}\text{Mn}_x$ (Refs. 16 and 17) and $\text{Sn}_{1-x}\text{Mn}_x$ (Ref. 17) thermopower of alloys measured with x between 0 and 0.7. With $\text{In}_{1-x}\text{Mn}_x$ we obtain a value of $+14 \mu\text{V } ^\circ\text{C}^{-1}$ while with $\text{Sn}_{1-x}\text{Mn}_x$ we obtain $+8 \mu\text{V } ^\circ\text{C}^{-1}$. For the three potentials, the calculated thermopower of manganese is very negative (near $-35 \mu\text{V } ^\circ\text{C}^{-1}$). It can be noticed that the generalized gradient correction does not improve the results of liquid manganese in the nonmagnetic phase. Even if one considers a relative inaccuracy of the Fermi energy determination, one can never obtain simultaneously a reasonable resistivity and thermopower.

The spin-dependent curves have been calculated within an atomic configuration following Hund's rule with five unpaired d electrons. The energy-dependent resistivity curves are represented in Fig. 4. The curves are broader and less prominent than for the spin-independent representations. Table II summarizes for comparison the same physical quantities as in Table I. These findings result from an electronic

TABLE I. Fermi energy E_F , effective number of conduction electrons N_C , resistivity $\rho(E_F)$, and thermopower $S(E_F)$ of liquid manganese. Calculations were made at 1260 °C using the Kohn-Sham (Ref. 12), the LDA (Ref. 6), and GGA-PBE (Ref. 7) potentials without spin effect.

Manganese 1260 °C	E_F (Ry.)	N_C	$\rho(E_F)$ ($\mu\Omega$ cm)	$S(E_F)$ ($\mu\text{V } ^\circ\text{C}^{-1}$)
Kohn-Sham	0.640	1.858	1430	-33.7
LDA	0.675	2.010	1206	-34.8
GGA-PBE	0.698	2.114	1051	-35.4
Experiment			205 ± 5 ¹⁴	-1 ± 2 ¹⁵

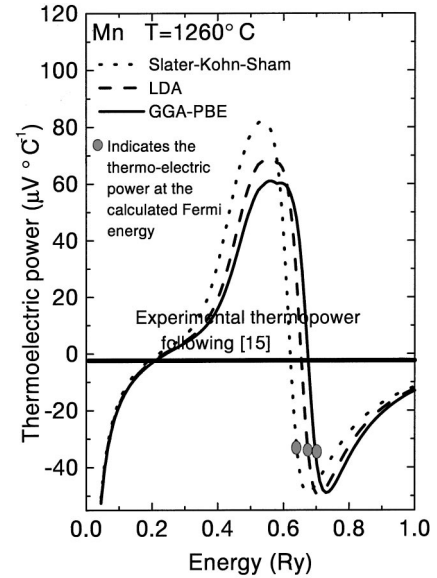


FIG. 3. Energy dependence of the thermopower of liquid manganese. Calculations were made at 1260 °C using the Kohn-Sham (Ref. 12), the LDA (Ref. 6), and GGA-PBE (Ref. 7) potentials without spin effect.

density of states that is more spread out as a consequence of the exchange splitting. The maximum of the PBE curve lies below the experimental value in contrast to the LDA maximum that is above. The thermopower is represented in Fig. 5. Both calculated values with our two density-functional theory (DFT) approximation are near $-12 \mu\text{V } ^\circ\text{C}^{-1}$. It becomes clearly apparent that the spin-dependent approach improves significantly the resistivity results and that for the thermopower the values move towards zero in the right way.

IV. DISCUSSION

Our spin-independent calculated resistivity including the sd contributions has a very large value with respect to the

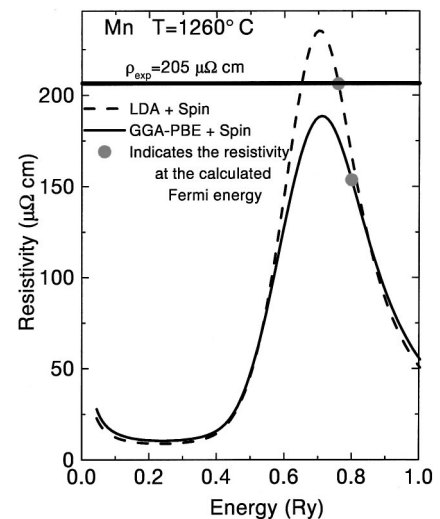


FIG. 4. Energy dependence of the electrical resistivity of liquid manganese at 1260 °C with the LDA (Ref. 6) and GGA-PBE (Ref. 7) potentials by including the spin effect with a magnetic moment of $5 \mu_B$.

TABLE II. Fermi energy E_F , effective number of conduction electrons N_C , resistivity $\rho(E_F)$, and thermopower $S(E_F)$, of liquid manganese. Calculations were made at 1260 °C using the Kohn-Sham (Ref. 12), the LDA (Ref. 6), and GGA-PBE (Ref. 7) potentials by including the spin effect (magnetic moment of $5\mu_B$).

Manganese 1260 °C	E_F (Ry.)	N_C	$\rho(E_F)$ ($\mu\Omega$ cm)	$S(E_F)$ ($\mu\text{V } ^\circ\text{C}^{-1}$)
LDA+spin	0.760	2.402	206	-12.0
GGA-PBE+spin	0.800	2.594	154	-11.5
Experiment			205 ± 5 ¹⁴	-1 ± 2 ¹⁵

experimental result. Taking into account the d resonance, similar high resistivities have been found by Esposito, Ehrenreich, and Gelatt⁴ for cobalt, iron, and copper in contrast to nickel for which they obtained a satisfactory agreement. On the opposite, neglecting the d electrons, Hirata *et al.*¹⁸ do not encounter the discrepancy between the calculated and measured resistivity values since the theoretical value of $188 \mu\Omega$ cm is close to the experimental one. Nevertheless their result faces a major objection, namely, the prominent weight of the d density of states at the Fermi level. Indeed the theoretical calculations of Bose, Jepsen, and Anderson¹⁹ showed that the $3d$ electrons dominate the conductivity. Also the magnetic susceptibility measurements of El-Hanany and Warren²⁰ points out that the paramagnetic behavior originates mainly from the spin of the $3d$ electrons. It appears that one cannot doubt the participation of the $3d$ electrons in the resistivity process. Unfortunately within the spin-independent approach the calculated resistivity is not in agreement with the experiment. The comparison between Tables I and II points out that the spin-polarized results represent a noticeable progress over the nonpolarized case. Since the spin-polarized results are different from the nonpolarized ones only for an imbalance between the majority and

minority spin, our approach points towards the existence of local magnetic moments. The appearance of local moments might be explained via two kinds of hypothesis. A possible explanation is to assume the existence of genuine local moments as a consequence of local short-range order in the liquid phase. The moments are supposed to be present in the solid state just below the transition temperature and not substantially perturbed during the melting. It implies a magnetic ordering for the high-temperature solid δ phase as found by the calculations⁵ and a liquid short-range order close to the solid one. Another possible explanation stems from the spin-density fluctuation theory developed by Moriya²¹ for paramagnetic spin metals. In that model the low temperature susceptibility is expressed in terms of temperature-enhanced spin susceptibility. At higher temperature the enhancement is reduced and gives rise under favorable conditions to Curie-Weiss susceptibility identical to that obtained for localized moments. The model thus predicts the formation of temperature-induced local moments due to spin fluctuations. For solid δ manganese the structure factor has not been measured but the experimental magnetic situation exhibits very close behavior for the solid and the liquid phases.²⁰ The measured magnetic susceptibility is decomposed into an enhanced Pauli susceptibility accounting for 75–80 % of the total susceptibility and a remainder orbital paramagnetic susceptibility. Further the authors in Ref. 20 emphasize the nearly magnetic character of liquid manganese. As also few changes in the density of states are observed over the melting transition the presence of localized moments is very likely in manganese at high temperatures. Their appearance is strongly suggested by the experimental findings and simultaneously supported by theoretical considerations.

The spin-polarized calculations have been performed within a free-atom configuration corresponding to a spin moment of $5\mu_B$. Figure 4 evidences that the experimental value can never be reached for the GGA energy-dependent resistivity curve in contrast to LDA energy-dependent resistivity curve. Now we focus only on the GGA approximation since it is a better approximation as regards the exchange correlation potential than the simple LDA. A cause of the discrepancy of our GGA results with respect to the experiment should be the neglect of the multiple-scattering term. This explanation can be discarded in view of the calculations performed by Nardi.²² Based on the results of iron the account for the multiple scattering in Lloyd's formula gives rise to a reduction of about 15% for the resistivity. If a correction of similar magnitude is assumed for Mn, it worsens the high spin configuration result and another explanation has to be proposed in order to reconcile the GGA results with the experimental findings. As a matter of fact the atoms in the liquid phase cannot be considered as independent like in a gas. The electrons feel an interacting potential that gives rise to a mean atomic configuration lowering the atomic moment as in a solid. Figure 6 shows the influence of the moment on the resistivity curves for the GGA approximation. The energy-resistivity curves are raised with respect to the decreasing spin-moment configuration. The same behavior holds for the LDA curves that are not recorded since they exceed in height the corresponding GGA curves. For low

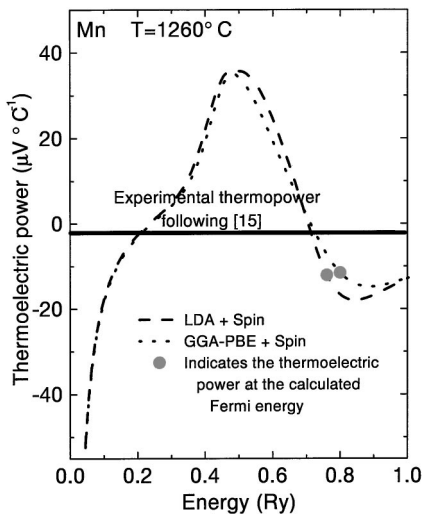


FIG. 5. Energy dependence of the thermopower of liquid manganese at 1260 °C with the LDA (Ref. 6) and GGA-PBE (Ref. 7) potentials by including the spin effect with a magnetic moment of $5\mu_B$.

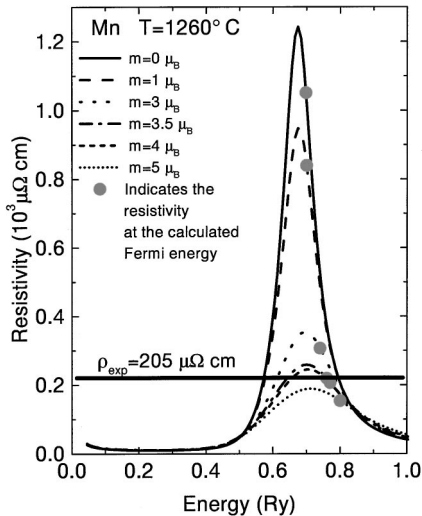


FIG. 6. Energy dependence of the electrical resistivity of liquid manganese at 1260 °C with the LDA (Ref. 6) and GGA-PBE (Ref. 7) potentials for different magnetic moments.

moments ranging between 0 and $1 \mu_B$ the GGA resistivity is far from the experimental values. With our Fermi energy determination, the experimental resistivity can be obtained for a moment varying between $3.5 \mu_B$ and $4 \mu_B$. The study confirms that the potential derived from the GGA approximation is the most appropriate for the transition metals. Further, our calculation furnishes estimation for the magnitude of the local moments. Within the Ziman approach the values for the moment in the liquid phase are found slightly above the calculated values for the solid δ phase.⁵

Examination of Fig. 7 representing the thermoelectric power curves indicates that the distance between the calculated and experimental values is considerably reduced with the spin-dependent calculation. The values at the Fermi energy are even too negative for all the simulated moments. However a shift of the Fermi energy downward lower energies about 0.05 Ry (for a moment between 3.5 and 4) fits on the experimental thermopower and stresses the fact that the quantity is very sensitive to the Fermi level position. The

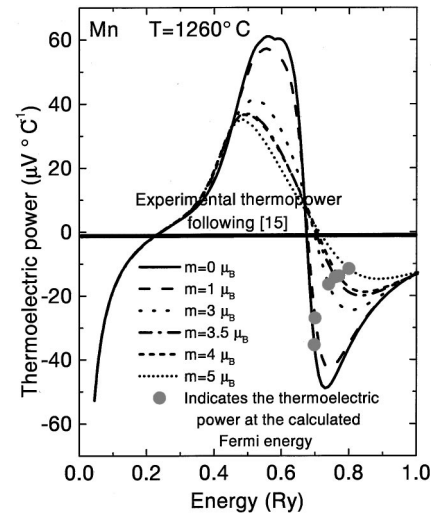


FIG. 7. Energy dependence of the thermopower of liquid manganese at 1260 °C with the LDA (Ref. 6) and GGA-PBE (Ref. 7) potentials for different magnetic moments.

same energy variation also affects the resistivity. One mean to overcome the difficulty is to better locate the Fermi energy. For instance with $m = 4.5 \mu_B$ and a shift of energy of -0.05 Ry one obtains both the experimental resistivity and thermopower. We believe that it could be realized by dropping our simple potential superposition model at the cost of a self-consistent density-of-states calculation.

V. CONCLUSION

The contribution of the $3d$ electrons to the resistivity is well established. Within the Ziman approach the spin-independent treatment leads to resistivity values far above the measured ones. The present study shows clearly that the spin-polarized approach improves substantially the results. These findings suggest the existence of local magnetic moments but further theoretical and experimental investigations should be put forward to clarify the magnetic situations of liquid manganese.

*Corresponding author. FAX: (33) 3 87 31 58 84. Email address: Gasser@lpli.sciences.univ-metz.fr

¹J. M. Ziman, *Philos. Mag.* **6**, 1013 (1961).

²R. Evans, D. A. Greenwood, and P. Lloyd, *Phys. Lett.* **35A**, 57 (1971).

³O. Dreirach, R. Evans, H. J. Güntherodt, and U. Künzi, *J. Phys. F: Met. Phys.* **2**, 709 (1972).

⁴E. Esposito, H. Ehrenreich, and C. D. Gelatt, *Phys. Rev. B* **18**, 3913 (1978).

⁵J. Kübler, *J. Magn. Magn. Mater.* **20**, 107 (1980).

⁶U. Von Barth and L. Hedin, *J. Phys. C* **5**, 1629 (1972).

⁷J. P. Perdew, K. Burke, and M. Ernzerhof, *Phys. Rev. Lett.* **77**, 3865 (1996).

⁸B. Delley and H. Beck, *J. Phys. F: Met. Phys.* **9**, 517 (1979).

⁹G. Mukhopadhyay, A. Jain, and V. K. Ratti, *Solid State Commun.* **13**, 1623 (1973).

¹⁰L. F. Mattheiss, *Phys. Rev. A* **133**, 1399 (1964).

¹¹J. C. Slater, *Phys. Rev.* **82**, 538 (1951).

¹²W. Kohn and L. Sham, *Phys. Rev. A* **140**, 1133 (1965).

¹³P. Lloyd, *Proc. Phys. Soc. Jpn.* **90**, 207 (1967).

¹⁴O. Tatsuya and O. Satow, *J. Phys. Soc. Jpn.* **55**, 599 (1986).

¹⁵M. V. Vedernikov, *Adv. Phys.* **18**, 337 (1969).

¹⁶H. Halim, Thèse de Doctorat, Université de Metz, 1991.

¹⁷C. Chaib, Thèse de Doctorat, Université de Metz, 1987.

¹⁸K. Hirata, Y. Waseda, A. Jain, and R. Srivastava, *J. Phys. F: Met. Phys.* **7**, 419 (1977).

¹⁹S. K. Bose, O. Jepsen, and O. K. Andersen, *Phys. Rev. B* **48**, 4265 (1993).

²⁰U. El-Hanany and W. W. Warren, Jr., *Phys. Rev. B* **12**, 861 (1974).

²¹T. Moriya, *Solid State Commun.* **26**, 483 (1978).

²²E. Nardi, *Phys. Rev. E* **54**, 1899 (1996).